Tetrahedron 65 (2009) 9626–9632

Contents lists available at ScienceDirect

Tetrahedron

journal homepage: www.elsevier.com/locate/tet

Triaryl linked donor acceptor dyads for high-performance dye-sensitized solar cells

Yuan Jay Chang [a], Tahsin J. Chow [a,b,*]

[a] Department of Chemistry, National Taiwan University, Taipei 106, Taiwan
[b] Institute of Chemistry, Academia Sinica, Taipei 115, Taiwan

ARTICLE INFO

Article history:
Received 31 August 2009
Accepted 8 September 2009
Available online 19 September 2009

ABSTRACT

The effect of changing substituents of organic dyes for their performance on dye-sensitized solar cells (DSSCs) is examined. These dyes consist of an aromatic amine donor group, a cyanoacrylic acid acceptor group, and a triaryl spacer group, while they are linked together by consecutive palladium catalyzed coupling reactions. These materials exhibit strong charge transfer absorption bands in the UV/vis region. Their redox potential levels were estimated by cyclic voltammetry, and found to suit well to the charge flow in DSSCs. Adding electron-donating substituents on the phenyl groups of aromatic amines increased the electron density on the donor groups, therefore reduced the HOMO/LUMO band gap. These dyes were chemisorbed on the surface of nanocrystalline TiO_2, and fabricated into DSSCs through standard operations. For a typical device the maximal monochromatic incident photon-to-current conversion efficiency (IPCE) can reach to 80%, with a short-circuit photocurrent density (J_{sc}) 16.34 mA cm^{-2}, an open-circuit photovoltage (V_{oc}) 0.68 V, and fill factor (FF) 0.55, which corresponds to an overall conversion efficiency of 6.05%.

1. Introduction

Ever since the report of Michael Grätzel in 1991 on a high-performance dye-sensitized solar cell (DSSC) made with Ru-complexes, researches in this area have boomed up very rapidly.[1] Nowadays the three landmark polypyridyl ruthenium(II) complexes, i.e., N3, N719, and the black dye, have achieved maximal power conversion efficiencies over 11%.[2] An enormous number of organic dyes have also been developed in this area, such as coumarin,[3] indoline,[4] cyanine,[5] merocyanine,[6] hemicyanine,[7] and porphyrin[8] derivatives, while most of them exhibited energy-to-electricity conversion efficiency within a range of 5–9%. Organic dyes possess an advantage of high structural flexibility, thus can be modified easily to compromise with other requirements necessary for optimizing the performance of DSSCs.

The quantum efficiency of DSSCs depends heavily on the electron transfer (ET) process, which happens immediately after photoexcitation. The rate of ET is governed by the free energy of the transition, which is related to the electronic potential levels of both the donors and the acceptors. It is anticipated that perturbing the potential energy levels of the donor groups by changing substituents may induce a substantial effect on the quantum efficiency of devices. In our previous studies we have investigated a series of organic donor–bridge–acceptor (D–B–A) dyads, in which a triarylamine donor group (D) and a cyanoacrylic acid acceptor group (A) are connected by a triaryl linkage (B).[9] These D–B–A dyads exhibited remarkable quantum efficiency while fabricated to DSSCs. Among a variety of different combinations, we have found that the B group made by combinations of phenyl–phenyl–thiophene (**PPS**) and phenyl–thiophene–phenyl (**PSP**) performed the best. The averaged quantum efficiency of devices made thereof ranged in 5–7%. In this report we tried to focus our efforts on these two types of structures, in the meanwhile to adjust the substituents on the triarylamine moiety in hope to promote the efficiency to a higher level. Although there have been abundant reports on various dye structures in the literatures, works aimed on the substituent effect were scant.[10] Results in this regard will certainly provide a useful reference to the future design of dye materials.

2. Results and discussion

The general formula of compounds prepared in this report is shown in Figure 1 and their synthetic sequences are outlined in Scheme 1. The synthesis started from diarylamine, on which the third aromatic substituent bearing a *p*-bromo group was introduced. A new C–N bond was built up through Buchwald–

* Corresponding author.
E-mail address: tjchow@chem.sinica.edu.tw (T.J. Chow).

0040-4020/$ – see front matter © 2009 Elsevier Ltd. All rights reserved.
doi:10.1016/j.tet.2009.09.036

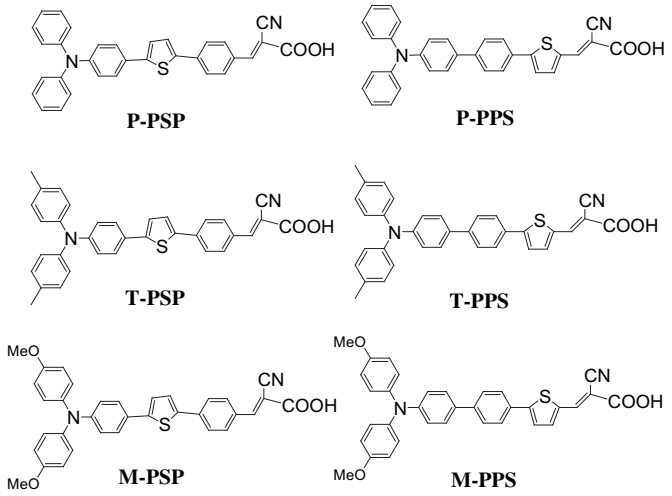

Figure 1. Organic dye structures of **PSP** and **PPS** series.

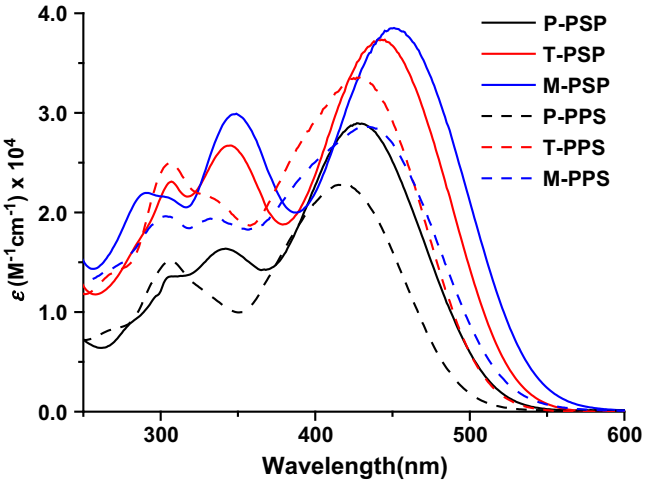

Figure 2. Absorption spectra of organic dyes in THF, where ε is molar extinction coefficient.

Hartwig coupling reaction catalyzed by $Pd(OAc)_2$. The structure of compounds **1** and **4** exhibited a twofold symmetry, which can be justified by their ^1H and ^{13}C NMR spectra. The extension of aryl chain in **1** was accomplished by Stille coupling reactions for adding a thiophenyl and a phenyl moiety subsequently. The yields of **2** and **3** were quite satisfactory, i.e., in a range of 68–85%. For compounds **4**, a 2-formylthiophenyl group was added on by Suzuki coupling reactions to yield **5** in 68–88% yields. The cyanoacrylic acid moiety was generated via Knoevenagel condensation by fusing up with a cyanoacetic acid as the final step. All final products can be crystallized into deep color solids.

band gaps. The major absorption band shifts from 427 nm to 445 and 451 nm for **P-PSP**, **T-PSP**, and **M-PSP**, respectively (Fig. 2). The effect may be ascribed to the ability of electron-denoting with the substituent, which increases the electron density on the triarylamine moiety. As a result the potential energy level of HOMO is elevated, therefore reduces the gap between HOMO and LUMO. The effect can also be detected experimentally by the reductive oxidation potentials along the series (Table 1).

Another phenomenon noteworthy in Figure 2 is that the absorption wavelength of **PSP** series compounds (solid lines) seems to

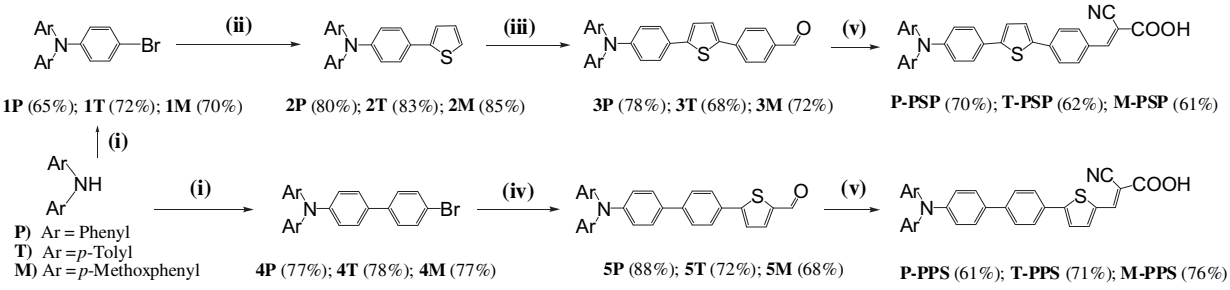

Scheme 1. Synthetic routes of organic dyes. Reagents: (i) $Pd(OAc)_2$/dppf, 1,4-dibromobenzene (for **1**) or 4,4′-dibromobiphenyl (for **4**), toluene, 90 °C; (ii) $PdCl_2(PPh_3)_2$, 2-(tributylstannyl)thiophene, DMF, 90 °C; (iii) BuLi, tributyltin chloride, THF, −78 °C; followed by $PdCl_2(PPh_3)_2$, 4-bromobenzaldehyde, DMF, 90 °C; (iv) (a) BuLi, triisopropylborate, THF, −78 °C; followed by $HCl_{(aq)}$, (b) $Pd(PPh_3)_4$, 5-bromothiophene-2-carbaldehyde, toluene, K_2CO_3, 90 °C; (v) cyanoacetic acid, NH_4OAc, AcOH, 90–100 °C.

The absorption spectra of organic dyes in THF solution are shown in Figure 2. Each of these compounds exhibits a major absorption band at λ_{max} 380–550 nm, which is assigned to a π–π^* transition. This band exhibits a mild solvent shift, indicating its dipolar characteristic. The HOMO level of the compounds is localized mostly at the triarylamine (D) moiety, while the LUMO at the cyanoacrylic acid (A). Upon photoexcitation an electron migrates from D to A, forming a charge-separated dipolar state. In both of the ground and excited states, the electron density of D and A is heavily coupled with the orbitals in the central triaryl linkage (B). The phenomenon can be clearly justified by observing the gradual spectral shift upon elongation of the chain length (Fig. 3). An approximate 50 nm bathochromic shift is observed with an extension of each aryl unit. Although more photons with lower energy can be harvested by compounds with a longer bridge, the quantum efficiency of DSSC did not increase proportionally to the chain length beyond three aryl groups.[11]

The methyl substituent in the T-series compounds (tolyl) and the methoxy substituent in the M-series (*p*-methoxyphenyl) compounds did exhibit an effect of narrowing down the HOMO/LUMO

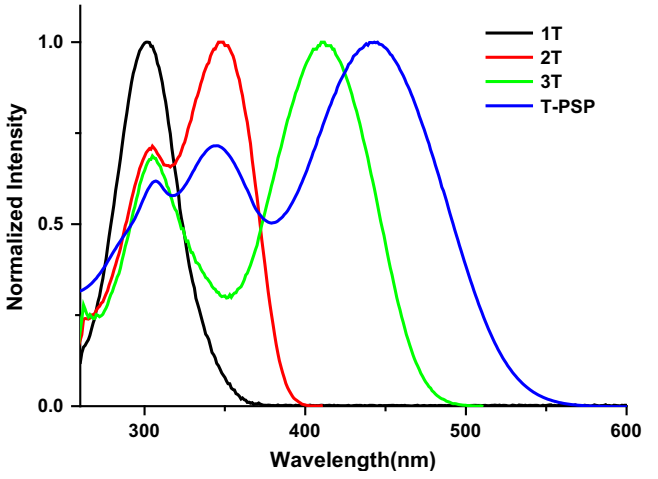

Figure 3. Absorption spectra of organic compounds **1T**, **2T**, **3T**, and **T-PSP** in THF. An approximate 50 nm bathochromic shift is observed with an extension of each aryl unit.

Table 1
Calculated (TDDFT/B3LYP) and experimental parameters for dyes **PSP** and **PPS** series

Dye	HOMO/LUMO[a] (eV)	Band gap[a]	f[a]	λ_{abs}[b] nm (ε/M^{-1} cm^{-1})	λ_{abs} nm (on TiO_2)	HOMO[c]/LUMO[d] (eV)	E_{ox}[e] (V)	E_{0-0}[f] (V)	E_{LUMO}[g] (V)	J_{sc} (mA cm^{-2})	V_{oc} (V)	FF	η[h] (%)
P-PSP	−5.06/−2.61	2.45	0.71	427(29,000)	399	−5.29/−2.77	0.79	2.53	−1.73	15.36	0.69	0.50	5.25
T-PSP	−4.96/−2.59	2.37	0.69	445(37,400)	416	−5.22/-2.76	0.72	2.46	−1.74	16.34	0.68	0.55	6.05
M-PSP	−4.78/−2.55	2.23	0.63	451(38,600)	427	−5.09/−2.71	0.59	2.38	−1.79	16.60	0.65	0.56	5.98
P-PPS	−5.09/−2.64	2.45	0.41	417(23,000)	399	−5.36/−2.82	0.86	2.54	−1.68	13.86	0.65	0.57	5.14
T-PPS	−4.97/−2.63	2.34	0.38	430(33,700)	406	−5.22/−2.71	0.72	2.51	−1.79	12.00	0.71	0.61	5.26
M-PPS	−4.79/−2.59	2.20	0.37	432(33,400)	416	−5.04/−2.60	0.54	2.44	−1.90	11.16	0.60	0.61	4.09
N719	—	—	—	—	—	—	—	—	—	17.68	0.75	0.61	7.64

f: Oscillator strength for the lowest energy transition; ε: absorption coefficient; E_{ox}: oxidation potential; E_{0-0}: 0–0 transition energy measured at the intersection of absorption and emission spectra; J_{sc}: short-circuit photocurrent density; V_{oc}: open-circuit photovoltage; FF: fill factor; η: total power conversion efficiency.
[a] TDDFT/B3LYP calculated values.
[b] Absorptions were measured in THF.
[c] Oxidation potentials of dyes (10^{-3} M) in THF containing 0.1 M $(n\text{-}C_4H_9)_4NPF_6$ with a scan rate of 100 mV s^{-1}.
[d] LUMO was calculated by HOMO−E_{0-0}.
[e] E_{ox} was calculated by HOMO+4.5 (eV) (vs NHE).
[f] E_{0-0} was determined from intersection of absorption and emission in THF.
[g] E_{LUMO} was calculated by $E_{ox}-E_{0-0}$.
[h] Performance of DSSC measured in a 0.25 cm^2 working area on an FTO (15 Ω/square) substrate.

be consistently longer than those of the **PPS** series (dotted lines). This can be explained by a more planar geometry in the former, because inserting a thiophenyl group between two phenyl rings effectively reduced the steric hindrance imposed by two adjacent phenyl groups. The better planarity of **PSP** compounds also lead to a higher oscillator strength for the lowest energy transition (Table 1). The measured molar extinction coefficients (2.3–3.9×10^4 M^{-1} cm^{-1}) of all compounds are not apparently different from each other, yet all higher than that of the well-known ruthenium dyes ($<2\times10^4$ M^{-1} cm^{-1}).

The absorption spectra of dyes, after they were chemisorbed onto the surface of TiO_2, displayed a mild blue shift with respect to those in solutions (S2). Such a phenomenon has been recognized before, and was attributed to the reduction of electron accepting ability of the cyanoacrylate group.[12] The rationale was supported by the observation of a similar blue shift in a more polar solvent (S1). The high polarity of the medium promoted a partial deprotonation of the carboxylic acid group. It is considered that the titanium carboxylate moiety possesses an electronic structure closer analogous to that of a deprotonated carboxylate than an acid group.[13] Another noteworthy feature in the spectra of the chemisorbed materials is an apparent tailing toward longer wavelength region (S2). In solutions the low energy edge of absorption bands does not exceed 600 nm (Fig. 2), yet on TiO_2 the absorption band extends beyond it. The long wavelength absorption can be ascribed to the formation of aggregates on the surface of TiO_2. The absorption of aggregates is responsible for the induction of photocurrent in the regions of ≥600 nm (Fig. 6).

In the ground state the three triaryl rings maintained nearly a coplanar conformation in order to achieve a maximal extent of π-delocalization. In the excited state, however, their conformation may be re-adjusted to a geometry quite different from the ground state. A straightforward way to detect such a geometrical change is to measure the Stokes shift between the absorption and emission spectra. All these dyes displayed fluorescence in organic solvents with low intensity. The emission spectra of certain dyes displayed an uncommon feature, i.e., abnormal broad bands with dual maxima (S3). As the formation of aggregates is unlikely in dilute solutions, the dual emissions were believed to derive from the excited state in different conformations, which exist in equilibrium with each other. The emission at longer wavelength is derived from the conformational isomer with a greater twist from the original geometry.

The first oxidation potentials (E_{ox}), corresponding to the HOMO level of dyes, were measured by cyclic voltammetry (CV) in THF, and the results are included in Table 1. The relative voltages decrease in the order of **P-PSP** (0.79)>**T-PSP** (0.72)>**M-PSP** (0.59), as well as **P-PPS** (0.86)>**T-PPS** (0.72)>**M-PPS** (0.54). The trend is consistent with the relative electron-donating ability of the substituents. The LUMO levels of sensitizer were estimated by the values of E_{ox} and the 0–0 band gaps, while the latter were obtained at the intersection of absorption and emission spectra. The band gap energies and the first oxidation potentials reduce along with the electron-donating power of the substituents in both series. The trends appear as: **P-PSP** (2.53)>**T-PSP** (2.46)>**M-PSP** (2.38) and **P-PPS** (2.54)>**T-PPS** (2.51)>**M-PPS** (2.44), respectively. The estimated LUMO levels of all dyes are sufficiently higher than the conductive band level of TiO_2 (ca. −0.5 V), while their HOMO levels are sufficiently lower than that of electrolyte pair I^-/I_3^- (ca. 0.4 V). The electronic structures thus ensure a favorable exothermic flow of charges throughout the photo-electronic conversion.

To gain insight in the electronic configurations, these compounds were further examined by theoretical models. The molecular geometries were optimized by using B3LYP/6-31G* basis set first, then the orbitals of both ground and excited states were computed by time-dependent density functional theory (TDDFT) with B3LYP functional implanted in a Gaussian 03 program. According to the optimized molecular geometry, the conformation of **PSP** bridge is nearly coplanar, but the orientation of two adjacent phenyl rings of a **PPS** bridge is twisted to ∼34° due to the steric hindrance (S5). The triarylamine moieties with electron-donating substituents displayed smaller energy gaps as well as lower oxidation potentials. As a result the molecular dipole moments of **M-PSP** and **T-PSP** are greater than that of **P-PSP**. The former also exhibits a higher molar extinction coefficient for a more efficient light harvesting. The calculated HOMO/LUMO energy levels and the corresponding band gaps are listed in Table 1, whereas they are remarkably consistent with the experimental values. The difference in Mulliken charge density surrounding D, B, and A segments, before (S_0 state) and after (S_1 state) the photoexcitation, can be more clearly depicted by the magnitude of bar charts (S4).

The electronic density distributions of HOMO and LUMO are illustrated in Figure 4. The electron density of HOMO is localized mainly on the triarylamine moiety, and is extended along the bridge to the central region of the molecule. Electronic delocalization along a **PSP** bridge is more extended comparing with a **PPS** bridge, as a result of more planar conformation. Upon photoexcitation, the lowest energy transition involves the migration of a electron from the HOMO to the LUMO, which is localized on the opposite sides of the structure. Substantial conformational readjustments are expected as a consequence. The conformation between adjacent aryl groups becomes more twisted, thus hinders

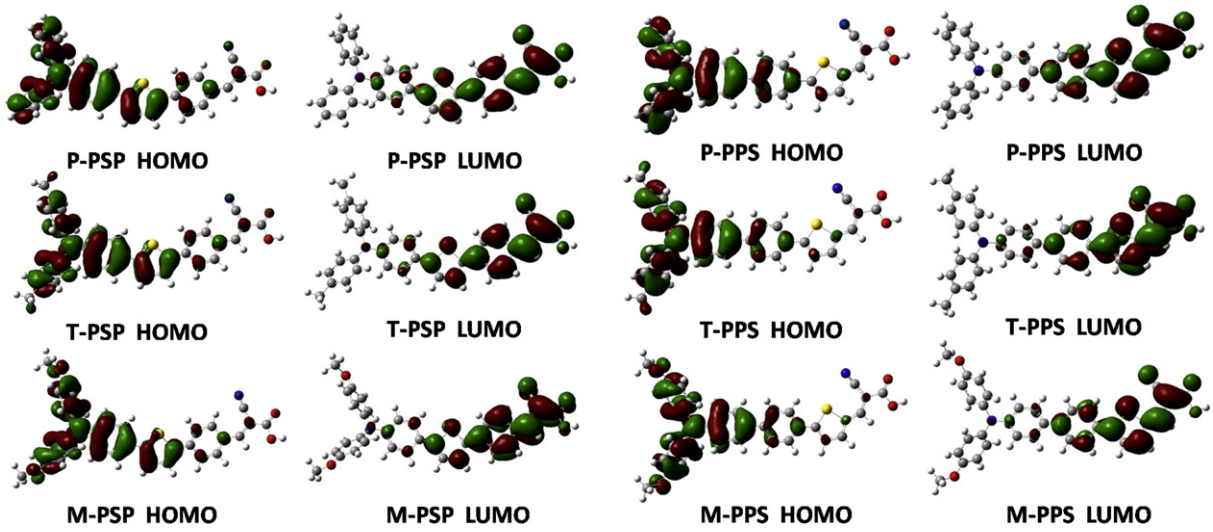

Figure 4. Computed frontier orbitals of dyes. The left graphs are the HOMOs, and the right ones are the LUMOs.

the charges to recombine. The quantum yield of solar conversion depends on both the amount of absorption (a larger extinction coefficient) and the rate of charge recombination (a long lifetime in the charge-separated state). In a combined effect the **PSP** bridge seems to perform better than **PPS** (Table 1).

The DSSC devices were fabricated by coating the dyes (3×10^{-4} M in THF) on the surface of nanocrystalline anatase TiO_2 with an effective area of 0.25 cm^2. A mixture of I_2 (0.05 M), LiI (0.5 M), and *tert*-butylpyridine (0.5 M) in acetonitrile solution was used as an electrolyte. The photovoltaic performance under a solar condition (AM 1.5) is listed in Table 1. The *J*–*V* curves of all dyes are shown in Figure 5. The current density of **PSP** series maintains a constant value in a range of 15–16 mA/cm^2, which was slightly better than those of **PPS** series in a range of 11–14 mA/cm^2. A comparison between the performances of **M-PSP** and **M-PPS** is worth mentioning. The former exhibited both a higher short-circuit current (J_{sc}=16.6 mA cm^{-2}) and a higher open-circuit voltage (V_{oc}=0.65 V) than the latter (J_{sc}=11.2 mA cm^{-2}; V_{oc}=0.60 V). The overall field factor (FF) of the former (0.56), however, was slightly smaller than that of the latter (0.61), which led to a relatively higher quantum efficiency (5.98% vs 4.09%). The presence of a thiophenylene unit in the center of the bridges in **M-PSP** improved its resonance delocalization with the triaryl moieties. All compounds of the **PSP** series performed slightly better than those of the **PPS** series. The best performance appears in **T-PSP**, which showed a maximal IPCE value 80% and an overall conversion efficiency 6.05%, quite compatible to the well-known ruthenium complex N719. The incident photon-to-current conversion efficiency (IPCE) was higher than 80% in 450–470 nm region. Plots of IPCE at various wavelengths are given in Figure 6. The photo-to-current conversion area of these dyes lay in the blue/green region, which matched with the highest region of solar emission.

In the process of fabricating the devices, we have noticed that for each dye the quantities to be coated on the surface of TiO_2 were slightly different. A quantitative comparison was done by examining the relative absorbance in THF before and after the dipping with a plate of TiO_2 (S8). The reduction of absorption intensity in the same solution is proportional to the amount taken away by the solid. The result indicated that the toluene derivatives, i.e., **T-PSP** and **T-PPS**, showed the maximal amounts of coating (S9). The coating quantity is therefore in parallel to the device performance, therefore is regarded to be a crucial parameter in our future studies.

In conclusion, the dye materials **PSP** and **PPS** have exhibited effective light-harvesting ability in DSSCs. The are several

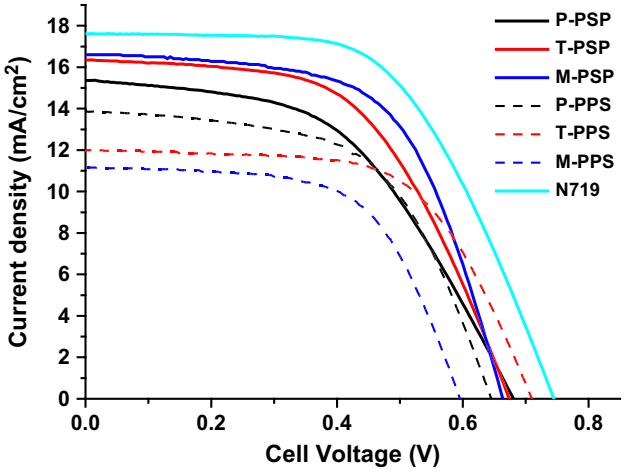

Figure 5. *J*–*V* curves of all dyes, with a comparison with N719.

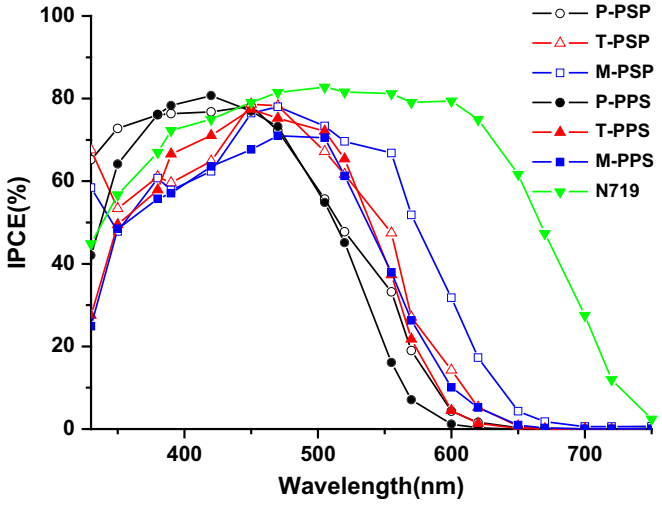

Figure 6. IPCE plots of all dyes, with a comparison with N719.

advantages preformed by these dyes: (1) handy preparation from low cost starting materials and purification without hazardous handlings; (2) large extinction coefficients in the visible region due to highly effective intramolecular charge transfer transitions; (3) stabilized charge-separated state, which diminishes dark-current in DSSC. The methyl and methoxy substituents showed an effect of narrowing down the HOMO/LUMO band gaps, therefore widen the light-harvesting region. The major absorption band shifts from 427 nm to 445 and 451 nm for **T-PSP** and **M-PSP**, respectively. The first oxidation potentials reduce along with the electron-donating power of the substituents. The estimated molecular dipole moment of **M-PSP** and **T-PSP** is greater than that of **P-PSP**. As a result the former exhibits higher molar extinction coefficient for a more efficient better light harvesting. The devices fabricated by using these materials display remarkable quantum efficiency, typically in a range of 4–6%. The optimal IPCE value reaches beyond 80%. The performance of **PSP** type compounds, in general, is slightly better than that of the **PPS** type. The presence of a thiophenylene in the center of **PSP** promotes better resonance delocalization. On the other hand, the twisted dihedral angles in **PPS** bridge may have the advantage of reducing the rate of charge recombination. The best performance among these compounds shows a J_{sc} value 16.34 mA cm^{-2}, V_{oc} value 0.68 V, and FF value 0.55, all summed up to an overall conversion efficiency 6.05%.

3. Experimental section

3.1. General information

All reactions were carried out under a nitrogen atmosphere. Solvents were distilled freshly according to standard procedures. ^{1}H and ^{13}C NMR spectra were recorded on a Bruker 400 MHz spectrometer. Absorption spectra were recorded on a Hewlett-Packard 8453 spectrofluorometer. The redox potentials were measured by using cyclic voltammetry on CHI 620 analyzer. Mass spectra were recorded on a VG70-250S mass spectrometer. Elementary analyses were performed on a Perkin–Elmer 2400 CHN analyzer. The starting materials diphenylamine, di-*p*-tolylamine, bis(4-methoxyphenyl)amine, 4,4′-dibromobiphenyl, 1,4-dibromobenzene, 4-bromobenzaldehyde, 5-bromothiophene-2-carbaldehyde, 2-(tributylstannyl)-thiophene, and cyanoacetic acid were purchased from ACROS, Merck, Lancaster, TCI, Sigma–Aldrich, and purified before use. Chromatographic separations were carried out on silica gel Merk Kieselgel si 60 (40–63 μm).

3.2. Fabrication and characterization of DSSCs

A thin film of TiO_2 (16–18 μm thick) was coated on a 0.25 cm^2 FTO glass substrate. It was immersed in a THF solution containing 3×10^{-4} M dye sensitizers for 12 h, then rinsed with anhydrous acetonitrile and dried. Another piece of FTO with sputtering 100 nm thick Pt was used as a counter electrode. The active area was controlled at a dimension of 0.25 cm^2 by adhering 60 μm thick polyester tape on the Pt electrode. The photocathode was placed on top of the counter electrode and was tightly clipped together to form a cell. Electrolyte was then injected into the seam between two electrodes. An acetonitrile solution containing LiI (0.5 M), I_2 (0.05 M), and 4-*tert*-butylpyridine (0.5 M) was used as the electrolyte. Devices made of a commercial dye N719 under the same condition was compared as a reference. The cell parameters were obtained under an incident light with intensity 100 mW cm^{-2}, which was generated by a 300 W Xe lamp passing through an AM 1.5 filter. The current–voltage parameters of DSSCs were recorded by a potentiostat/galvanostat model CHI650B (CH Instruments, USA).

3.3. Quantum chemistry computation

The structures of dye were optimized by using B3LYP/6-31G* hybrid functional. For the excited states, a time-dependent density functional theory (TDDFT) with the B3LYP functional was employed. All analyses were performed under Q-Chem 3.0 software. The frontier orbital plots of HOMO and LUMO were drawn by using Gaussian 03.

*3.3.1. (E)-2-Cyano-3-(p-(5′-(p-dimethoxyphenylamino)-phenyl)-thiophen-2′-yl)phenylacrylic acid (**M-PSP**).* A mixture of **3M** (250 mg, 0.51 mmol), cyanoacetic acid (52 mg, 0.61 mmol), and ammonium acetate (10 mg, 0.13 mmol) in acetic acid was placed in a three-necked flask under a nitrogen atmosphere and was stirred at 90–100 °C for 12 h. After cooling, the reaction was quenched by adding distilled water, and extracted with CH_2Cl_2. The organic layer was dried over anhydrous $MgSO_4$ and evaporated under vacuum. The product was purified by silica gel column chromatograph eluted with CH_2Cl_2/acetic acid (19/1). The orange solid was isolated in 61% yield (174 mg, 0.31 mmol), mp: 221–222 °C. ^{1}H NMR (DMSO-d_6): δ 8.17 (s, 1H), 7.99 (d, 2H, J=8.4 Hz), 7.78 (d, 2H, J=8.4 Hz), 7.64 (d, 1H, J=3.8 Hz), 7.47 (d, 2H, J=8.6 Hz), 7.35 (d, 1H, J=3.8 Hz), 7.01 (d, 4H, J=8.9 Hz), 6.89 (d, 4H, J=8.9 Hz), 6.73 (d, 2H, J=8.6 Hz), 3.70 (s, 6H); ^{13}C NMR (DMSO-d_6): δ 164.2, 156.4, 152.1, 148.7, 145.5, 139.9, 139.7, 137.8, 131.6, 130.7, 127.4, 127.3, 126.6, 125.5, 125.0, 123.9, 119.3, 117.5, 115.4, 105.3, 55.64. HRMS (m/z): 558.1605 (M$^+$). Anal. Calcd for ($C_{34}H_{26}N_2O_4S$): C, 73.10; H, 4.69; N, 5.01; O, 11.46; S, 5.74, found C, 73.06; H, 4.70; N, 4.97; O, 11.51; S, 5.76.

*3.3.2. (E)-2-Cyano-3-(p-(5′-(p-diphenylamino)phenyl)-thiophen-2′-yl)phenylacrylic acid (**P-PSP**).* Compound **P-PSP** was synthesized according to the same procedure as that of **M-PSP**. Orange solid of **P-PSP** was obtained in 70% yield, mp: 262–264 °C. ^{1}H NMR (DMSO-d_6): δ 8.22 (s, 1H), 7.80 (d, 1H, J=3.7 Hz), 7.77 (d, 2H, J=8.3 Hz), 7.71 (d, 2H, J=8.3 Hz), 7.67 (d, 1H, J=3.7 Hz), 7.62 (d, 2H, J=8.5 Hz), 7.30 (t, 4H, J=7.6 Hz), 6.99–7.06 (m, 8H); ^{13}C NMR (DMSO-d_6): δ 164.2, 149.1, 147.5, 147.3, 140.3, 137.6, 136.2, 133.1, 131.6, 130.0, 127.9, 127.2, 126.8, 124.9, 124.7, 123.8, 123.4, 119.1. HRMS (m/z): 498.1395 (M$^+$) (calcd for $C_{32}H_{22}N_2O_2S$: 498.1402). Anal. Calcd for $C_{32}H_{22}N_2O_2S$: C, 77.09; H, 4.45; N, 5.62; O, 6.42; S, 6.43, found C, 77.03; H, 4.51; N, 5.57; O, 6.49; S, 6.40.

*3.3.3. (E)-2-Cyano-3-(p-(5′-(p-ditolylamino)phenyl)thiophen-2′-yl)-phenylacrylic acid (**T-PSP**).* Compound **T-PSP** was synthesized according to the same procedure as that of **M-PSP**. Black solid of **T-PSP** was obtained in 62% yield, mp: 252–254 °C. ^{1}H NMR (DMSO-d_6): δ 8.24 (s, 1H), 8.02 (d, 2H, J=8.4 Hz), 7.81 (d, 2H, J=8.4 Hz), 7.67 (d, 1H, J=3.8 Hz), 7.52 (d, 1H, J=8.6 Hz), 7.39 (d, 1H, J=3.8 Hz), 7.10 (d, 4H, J=8.4 Hz), 6.91 (d, 4H, J=8.32 Hz), 6.85 (d, 2H, J=8.6 Hz), 2.23 (s, 6H); ^{13}C NMR (DMSO-d_6): δ 163.8, 153.5, 148.1, 145.4, 144.6, 140.0, 138.2, 133.3, 132.0, 130.5, 130.5, 127.7, 126.8, 126.3, 125.6, 125.1, 124.4, 121.6, 116.8, 103.2, 20.8. HRMS (m/z): 526.1712 (M$^+$). Anal. Calcd: C, 77.54; H, 4.98; N, 5.32; O, 6.08; S, 6.09, found C, 77.47; H, 5.02; N, 5.30; O, 6.10; S, 6.11.

*3.3.4. (E)-2-Cyano-3-(5′-(dimethoxyphenylaminobiphenylene)-thiophen-2′-yl)acrylic acid (**M-PPS**).* Compound **M-PPS** was synthesized according to the same procedure as that of **M-PSP**. Red solid of **M-PPS** was obtained in 76% yield, mp: 270–272 °C. ^{1}H NMR (DMSO-d_6): δ 8.46 (s, 1H), 7.98 (d, 1H, J=3.8 Hz), 7.78 (d, 2H, J=8.1 Hz), 7.75 (d, 1H, J=3.8 Hz), 7.68 (d, 2H, J=8.2 Hz), 7.54 (d, 2H, J=8.4 Hz), 7.03 (d, 4H, J=8.7 Hz), 6.90 (d, 4H, J=8.7 Hz), 6.80 (d, 2H, J=8.4 Hz), 3.72 (s, 6H); ^{13}C NMR (DMSO-d_6): δ 164.0, 156.3, 152.9, 148.8, 146.8, 141.7, 141.2, 140.1, 134.7, 130.7, 130.4, 127.6, 127.3, 127.1, 126.9, 125.3, 119.5, 116.9, 115.4, 98.8, 55.6. HRMS (m/z): 558.1612 (M$^+$). Anal. Calcd for

($C_{34}H_{26}N_2O_4S$): C, 73.10; H, 4.69; N, 5.01; O, 11.46; S, 5.74, found C, 73.11; H, 4.72; N, 4.97; O, 11.49; S, 5.71.

*3.3.5. (E)-2-Cyano-3-(5′-(diphenylaminobiphenylene)thiophen-2′-yl) acrylic acid (**P-PPS**).* Compound **P-PPS** was synthesized according to the same procedure as that of **M-PSP**. Black solid of **P-PPS** was obtained in 61% yield, mp: 267–269 °C. ^{1}H NMR (DMSO-d_6): δ 8.05 (s, 1H), 7.95 (d, 2H, J=7.4 Hz), 7.80 (d, 2H, J=8.2 Hz), 7.66 (d, 1H, J=3.7 Hz), 7.59 (d, 2H, J=8.7 Hz), 7.44 (d, 1H, J=3.8 Hz), 7.31 (t, 4H, J=7.9 Hz), 7.02–7.08 (m, 6H), 6.96 (d, 2H, J=8.7 Hz); ^{13}C NMR (DMSO-d_6): δ 164.3, 148.3, 147.5, 147.1, 144.4, 140.8, 136.4, 132.0, 130.8, 130.0, 127.5, 126.9, 126.8, 125.6, 124.8, 124.6, 123.9, 123.2, 119.1. HRMS (m/z): 498.1395 (M^+) (calcd for $C_{32}H_{22}N_2O_2S$: 498.1402). Anal. Calcd for $C_{32}H_{22}N_2O_2S$: C, 77.09; H, 4.45; N, 5.62; O, 6.42; S, 6.43, found C, 77.13; H, 4.49; N, 5.59; O, 6.45; S, 6.34.

*3.3.6. (E)-2-Cyano-3-(5′-(ditolylaminobiphenylene)thiophen-2′-yl)-acrylic acid (**T-PPS**).* Compound **T-PPS** was synthesized according to the same procedure as that of **M-PSP**. Red solid of **T-PPS** was obtained in 71% yield, mp: 262–264 °C. ^{1}H NMR (DMSO-d_6): δ 8.42 (s, 1H), 7.94 (d, 1H, J=4.0 Hz), 7.75 (d, 2H, J=8.3 Hz), 7.71 (d, 1H, J=4.0 Hz), 7.66 (d, 2H, J=8.3 Hz), 7.53 (d, 2H, J=8.6 Hz), 7.07 (d, 4H, J=8.2 Hz), 6.90 (d, 6H, J=8.3 Hz), 2.23 (s, 6H); ^{13}C NMR (DMSO-d_6): δ 164.1, 152.5, 148.0, 146.4, 144.7, 141.3, 140.9, 134.9, 133.0, 131.8, 130.9, 130.5, 127.7, 127.0, 127.0, 125.2, 125.0, 121.9, 117.1, 99.6, 20.8. HRMS (m/z): 526.1710 (M^+).

*3.3.7. p-Bromo-N,N-dimethoxyphenylaniline (**1M**).* A mixture of 1,4-dibromobenzene (20.3 g, 87.0 mmol), $Pd(OAc)_2$ (540 mg, 0.58 mmol), dppf (800 mg, 1.45 mmol), bis(4-methoxyphenyl)-amine (6.65 g, 29.0 mmol), and sodium *tert*-butoxide (4.20 g, 43.5 mmol) in dry toluene was placed in a three-necked flask under a nitrogen atmosphere and was stirred at 90 °C for 15 h. After cooling, the reaction was quenched by adding water, then was extracted with ethyl acetate. The organic layer was dried over anhydrous $MgSO_4$ and evaporated under vacuum. The product was purified by silica gel column chromatograph eluted with hexane. White solid of **1M** was obtained in 70% yield (7.8 g, 20.3 mmol). ^{1}H NMR ($CDCl_3$): δ 7.23 (d, 2H, J=8.9 Hz), 7.03 (d, 4H, J=8.9 Hz), 6.82 (d, 2H, J=8.9 Hz), 6.78 (d, 2H, J=8.9 Hz), 3.79 (s, 6H); ^{13}C NMR ($CDCl_3$): δ 156.0, 147.8, 140.5, 131.7, 126.5, 121.9, 114.7, 112.3, 55.4. HRMS (m/z): 383.0512 (M^+).

*3.3.8. p-Bromo-N,N-diphenylaniline (**1P**).* Compound **1P** was synthesized according to the same procedure as that of **1M**. White solid of **1P** was obtained in 65% yield. ^{1}H NMR ($CDCl_3$): δ 7.32 (t, 2H, J=8.8 Hz), 7.20–7.29 (m, 4H), 7.05 (t, 4H, J=7.3 Hz), 6.96–7.02 (m, 2H), 6.90–6.93 (m, 2H); ^{13}C NMR ($CDCl_3$): δ 147.3, 146.9, 132.1, 129.3, 125.0, 124.3, 123.1, 114.7. HRMS (m/z): 323.0309 (M^+).

*3.3.9. p-Bromo-N,N-ditolylaniline (**1T**).* Compound **1T** was synthesized according to the same procedure as that of **1M**. White solid of **1T** was obtained in 72%. ^{1}H NMR ($CDCl_3$): δ 7.27 (d, 2H, J=8.9 Hz), 7.06 (d, 4H, J=8.4 Hz), 6.97 (d, 4H, J=8.4 Hz), 6.89 (d, 2H, J=8.8 Hz), 2.31 (s, 6H); ^{13}C NMR ($CDCl_3$): δ 147.4, 144.9, 132.8, 131.8, 129.9, 124.6, 123.8, 113.5, 20.8. HRMS (m/z): 351.0631 (M^+).

*3.3.10. N,N-Dimethoxyphenyl-p-(2′-thiophenyl)aniline (**2M**).* To a three-necked flask containing the mixture of **1M** (2.37 g, 6.19 mmol), $PdCl_2(PPh_3)_2$ (0.13 g, 0.18 mmol), and 2-tributylstannylthiophene (5.3 mL, 14.2 mmol) was added DMF (20 mL). The reaction mixture was stirred at 90 °C for 24 h. After cooling, the reaction was quenched by adding MeOH and $KF_{(aq)}$ (saturated 15 mL). The mixture was extracted with CH_2Cl_2 and the organic layer dried over anhydrous $MgSO_4$. Evaporation of the solvent gave the crude, which was purified by silica gel with hexane as eluent. White solid of **2M** was obtained in 85% yield (2.04 g, 5.26 mmol). ^{1}H NMR ($CDCl_3$): δ 7.43 (d, 2H, J=8.6 Hz), 7.17–7.18 (m, 2H), 7.09 (d, 4H, J=8.9 Hz), 7.03 (d, 1H, J=3.6 Hz), 7.02 (d, 1H, J=3.6 Hz), 6.95 (d, 2H, J=8.6 Hz), 6.85 (d, 4H, J=8.9 Hz), 3.81 (s, 6H); ^{13}C NMR ($CDCl_3$): δ 155.9, 148.1, 144.6, 140.7, 128.9, 127.9, 126.6, 126.3, 123.5, 121.7, 120.6, 114.6, 55.4. HRMS (m/z): 387.1283 (M^+).

*3.3.11. N,N-Diphenyl-p-(2′-thiophenyl)aniline (**2P**).* Compound **2P** was synthesized according to the same procedure as that of **2M**. White solid of **2P** was obtained in 80%. ^{1}H NMR ($CDCl_3$): δ 7.46 (d, 2H, J=8.6 Hz), 7.25 (d, 2H, J=7.5 Hz), 7.24 (d, 2H, J=7.4 Hz), 7.19–7.21 (m, 2H), 7.10 (d, 4H, J=7.5 Hz), 7.05 (d, 2H, J=8.4 Hz), 7.00–7.03 (m, 3H); ^{13}C NMR ($CDCl_3$): δ 147.4, 147.1, 144.2, 129.2, 128.5, 127.9, 126.6, 124.4, 123.9, 123.7, 122.9, 122.1. HRMS (m/z): 327.1084 (M^+).

*3.3.12. N,N-Ditolyl-p-(2′-thiophenyl)aniline (**2T**).* Compound **2T** was synthesized according to the same procedure as that of **2M**. White solid of **2T** was obtained in 83%. ^{1}H NMR ($CDCl_3$): δ 7.44 (d, 2H, J=8.7 Hz), 7.20 (d, 2H, J=4.3 Hz), 7.01–7.09 (m, 11H), 2.33 (s, 6H); ^{13}C NMR ($CDCl_3$): δ 147.6, 145.0, 144.4, 132.6, 129.8, 127.8, 127.6, 126.5, 124.6, 123.6, 122.5, 121.9, 20.7. HRMS (m/z): 355.1405 (M^+).

*3.3.13. p-(5-(p-(Dimethoxyphenylamino)phenyl)thiophen-2-yl)-benzaldehyde (**3M**).* A three-necked flask containing a mixture of **2M** (4.80 g, 12.4 mmol) in dry THF was adding dropwise BuLi (10 mL, 16.1 mmol, 1.6 M in hexane) at −78 °C, and the solution was allowed to warm up gradually to 0 °C for ca. 30 min. The solution was cooled again to −78 °C and to it was added dropwise tri-*n*-butylchlorostannane (5.3 mL, 16.1 mmol). The reaction was warmed up to room temperature and stirred overnight. The reaction mixture was quenched by the addition of water, and was extracted with CH_2Cl_2. The combined organic solution was dried over anhydrous $MgSO_4$, and dried under vacuum. The crude product was dissolved in dry DMF, then added *p*-bromobenzaldehyde (2.28 g, 12.38 mmol) and $PdCl_2(PPh_3)_2$ (237 mg, 0.37 mmol). The solution was heated to 90 °C for 24 h and then cooled. The reaction was quenched by the addition of MeOH and $KF_{(aq)}$ (saturated 15 mL). The mixture was extracted with CH_2Cl_2, while the organic layer was dried over anhydrous $MgSO_4$. Evaporation of the solvent gave a product, which was purified by silica gel column chromatography eluted with CH_2Cl_2/hexane (1/1). Compound **3M** was obtained in 72% yield (4.38 g, 8.9 mmol) as yellow solid. ^{1}H NMR ($CDCl_3$): δ 9.96 (s, 1H), 7.84 (d, 2H, J=7.7 Hz), 7.72 (d, 2H, J=7.7 Hz), 7.41 (d, 2H, J=8.0 Hz), 7.38 (d, 1H, J=3.9 Hz), 7.17 (d, 1H, J=2.5 Hz), 7.06 (d, 4H, J=8.0 Hz), 6.90 (d, 2H, J=8.0 Hz), 6.83 (d, 4H, J=8.1 Hz), 3.78 (s, 6H); ^{13}C NMR ($CDCl_3$): δ 191.3, 156.1, 148.7, 146.3, 140.3, 140.1, 140.0, 134.6, 130.4, 126.8, 126.3, 126.0, 125.6, 125.3, 122.8, 120.0, 114.7, 55.4. HRMS (m/z): 491.1561 (M^+).

*3.3.14. p-(5-(p-(Diphenylamino)phenyl)thiophen-2-yl)benzaldehyde (**3P**).* Compound **3P** was synthesized according to the same procedure as that of **2M**. Yellow solid of **3P** was obtained in 78%. ^{1}H NMR ($CDCl_3$): δ 10.00 (s, 1H), 7.89 (d, 2H, J=8.5 Hz), 7.76 (d, 2H, J=8.3 Hz), 7.51 (d, 2H, J=8.7 Hz), 7.43 (d, 1H, J=3.8 Hz), 7.27–7.31 (m, 4H), 7.24 (d, 1H, J=3.8 Hz), 7.05–7.10 (m, 8H); ^{13}C NMR ($CDCl_3$): δ 191.3, 147.8, 147.2, 145.9, 140.61, 140.1, 134.8, 130.4, 129.3, 127.5, 126.5, 126.0, 125.4, 124.6, 123.4, 123.3, 123.2. HRMS (m/z): 431.1342 (M^+).

*3.3.15. p-(5-(p-(Ditolylamino)phenyl)thiophen-2-yl)benzaldehyde (**3T**).* Compound **3T** was synthesized according to the same procedure as that of **3M**. Yellow solid of **3T** was obtained in 68%. ^{1}H NMR ($CDCl_3$): δ 9.96 (s, 1H), 7.85 (d, 2H, J=8.0 Hz), 7.73 (d, 2H, J=8.0 Hz), 7.43 (d, 2H, J=8.1 Hz), 7.39 (dd, 1H, J=3.6, 0.9 Hz), 7.19 (dd, 1H, J=3.6, 0.9 Hz), 7.07 (d, 4H, J=8.1 Hz), 6.99–7.02 (m, 6H), 2.31 (s, 6H); ^{13}C NMR ($CDCl_3$): δ 191.3, 148.2, 146.2, 144.7, 140.3, 140.1,

134.7, 133.0, 130.4, 129.9, 126.5, 126.3, 126.0, 125.4, 124.9, 123.1, 121.9, 20.8. HRMS (m/z): 459.1666 (M^+).

*3.3.16. 4-Bromo-4′-dimethoxyphenylaminobiphenyl (**4M**).* Compound **4M** was synthesized according to the same procedure as that of **1M**. White solid of **4M** was obtained in 77%. ^{1}H NMR ($CDCl_3$): δ 7.52 (d, 1H, J=8.5 Hz), 7.42 (d, 2H, J=8.6 Hz), 7.40 (d, 2H, J=8.6 Hz), 7.04–7.10 (m, 10H), 3.79 (s, 6H); ^{13}C NMR (100 MHz, $CDCl_3$): δ 147.9, 145.0, 139.6, 132.8, 132.6, 131.7, 129.9, 128.1, 127.3, 124.8, 122.4, 120.6, 55.4. HRMS (m/z): 459.0838 (M^+).

*3.3.17. 4-Bromo-4′-diphenylaminobiphenyl (**4P**).* Compound **4P** was synthesized according to the same procedure as that of **1M**. Yellow solid of **4P** was obtained in 77%. ^{1}H NMR ($CDCl_3$): δ 7.52 (d, 2H, J=8.6 Hz), 7.42 (dd, 4H, J=8.7, 1.3 Hz), 7.26 (dd, 4H, J=6.8, 1.8 Hz), 7.12 (dt, 6H, J=8.7, 1.8 Hz), 7.02 (d, 2H, J=7.3 Hz); ^{13}C NMR ($CDCl_3$): δ 147.5, 139.5, 133.5, 131.7, 129.3, 129.2, 128.1, 127.4, 124.5, 124.3, 123.6, 123.0, 120.8. HRMS (m/z): 399.0633 (M^+).

*3.3.18. 4-Bromo-4′-ditolylaminobiphenyl (**4T**).* Compound **4T** was synthesized according to the same procedure as that of **1M**. White solid of **4T** was obtained in 78%. ^{1}H NMR (400 MHz, $CDCl_3$): δ 7.52 (d, 1H, J=8.4 Hz), 7.42 (d, 2H, J=8.6 Hz), 7.40 (d, 2H, J=8.6 Hz), 7.04–7.10 (m, 10H), 2.35 (s, 6H); ^{13}C NMR (100 MHz, $CDCl_3$): δ=147.9, 145.0, 139.6, 132.8, 132.6, 131.7, 129.9, 128.1, 127.3, 124.8, 122.4, 120.6, 20.8. HRMS (m/z): 427.0942 (M^+).

*3.3.19. 5-(Dimethoxyphenylaminobiphenylene)thiophene-2-carbaldehyde (**5M**).* A three-necked round-bottom flask containing **4M** (6.99 g, 15.2 mmol) was added dropwise BuLi (10 mL, 16.1 mmol, 1.6 M in hexane) in dry THF at −78 °C, after then solution was brought to 0 °C and was stirred by a magnetic bar for 30 min. The solution was cooled again to −78 °C and to it was added dropwise triisopropylborate (5.3 mL, 19.8 mmol). The reaction was warmed up gradually to room temperature and was stirred overnight. To the reaction was then added excess amount of 10% $HCl_{(aq)}$ (30 mL), while the mixture was stirred for another 1 h. The reaction was quenched by pouring into distilled water, followed by extraction with ethyl acetate. The organic layer was dried over anhydrous $MgSO_4$. Evaporation of the solvent gave a crude product, which was immediately subjected to the next reaction. It was mixed with 5-bromothiophene-2-carbaldehyde (2.67 g, 14.0 mmol), $K_2CO_{3(aq)}$ (2.76 g, 2 mmol) in 10 mL H_2O, and $Pd(PPh_3)_4$ (807 mg, 0.69 mmol) in dry toluene/THF (2/1). The mixture was heated to 90 °C for 12 h. After cooling, the products were extracted with ethyl acetate and the organic layer dried over anhydrous $MgSO_4$. The crude product was dried under vacuum, and was purifies by silica gel column chromatograph eluted with CH_2Cl_2/hexane (1/1). Yellow solid of **5M** was obtained in 68% yield (5.08 g, 10.3 mmol). ^{1}H NMR ($CDCl_3$): δ 9.89 (s, 1H), 7.74 (d, 1H, J=4.0 Hz), 7.71 (d, 2H, J=8.2 Hz), 7.62 (d, 2H, J=8.2 Hz), 7.41 (d, 1H, J=4.0 Hz), 7.05–7.08 (m, 10H), 3.81 (s, 6H); ^{13}C NMR ($CDCl_3$): δ 182.6, 154.1, 148.1, 144.9, 142.1, 141.7, 137.4, 132.9, 132.3. 131.1, 129.9, 127.3, 126.9, 126.7, 124.8, 123.7, 122.1, 57.4. HRMS (m/z): 491.1551 (M^+).

*3.3.20. 5-(Diphenylaminobiphenylene)thiophene-2-carbaldehyde (**5P**).* Compound **5P** was synthesized according to the same procedure as that of **5M**. Yellow solid of **5M** was obtained in 88% yield. ^{1}H NMR ($CDCl_3$): δ 9.89 (s, 1H), 7.74 (d, 1H, J=3.9 Hz), 7.72 (d, 2H, J=8.4 Hz), 7.63 (d, 2H, J=8.4 Hz), 7.50 (d, 2H, J=8.6 Hz), 7.42 (d, 1H, J=3.9 Hz), 7.25–7.30 (m, 4H), 7.13–7.15 (m, 6H), 7.05 (t, 2H, J=7.3 Hz); ^{13}C NMR ($CDCl_3$): δ 182.0, 154.0, 147.7, 147.4, 142.1, 141.6, 137.4, 133.3, 131.3, 129.3, 127.5, 127.1, 126.7, 124.6, 123.8, 123.4, 123.1. HRMS (m/z): 431.1349 (M^+).

*3.3.21. 5-(Ditolylaminobiphenylene)thiophene-2-carbaldehyde (**5T**).* Compound **5T** was synthesized according to the same procedure as that of **5M**. Yellow solid of **5T** was obtained in 72%. ^{1}H NMR ($CDCl_3$): δ 9.89 (s, 1H), 7.74 (d, 1H, J=4.0 Hz), 7.71 (d, 2H, J=8.2 Hz), 7.62 (d, 2H, J=8.2 Hz), 7.41 (d, 1H, J=4.0 Hz), 7.05–7.08 (m, 10H), 2.33 (s, 6H); ^{13}C NMR (100 MHz, $CDCl_3$): δ 182.6, 154.1, 148.1, 144.9, 142.1, 141.7, 137.4, 132.9, 132.3, 131.1, 129.9, 127.3, 126.9, 126.7, 124.8, 123.7, 122.1, 20.7. HRMS (m/z): 459.1646 (M^+).

Acknowledgements

This work was supported by the National Science Council and Academia Sinica in Taiwan.

Supplementary data

Absorption and emission spectra in various solvents and on TiO_2. TDDFT calculated molecular geometries, Mulliken charges, and low energy transitions. Oxidative voltammograms of selected compounds and their estimated HOMO/LUMO levels. Relative absorbed amounts on TiO_2. ^{1}H and ^{13}C NMR spectra of all compounds. Supplementary data associated with this article can be found in online version at doi:10.1016/j.tet.2009.09.036.

References and notes

1. O'Regan, B.; Grätzel, M. *Nature (London)* **1999**, *352*, 737.
2. (a) Nazeeruddin, M. K.; Key, A.; Rodicio, I.; Humphry-Baker, R.; Müller, E.; Liska, P.; Vlachopoulous, N.; Grätzel, M. *J. Am. Chem. Soc.* **1993**, *115*, 6382; (b) Nazeeruddin, M. K.; Zakeeruddin, S. M.; Humphry-Baker, R.; Jirousek, M.; Liska, P.; Vlachopoulous, N.; Shklover, V.; Fischer, C. H.; Grätzel, M. *Inorg. Chem.* **1999**, *38*, 6298; (c) Nazeeruddin, M. K.; Péchy, P.; Renouard, T.; Zakeeruddin, S. M.; Humphry-Baker, R.; Comte, P.; Liska, P.; Cevey, L.; Costa, E.; Shklover, V.; Spiccia, L.; Deacon, G. B.; Bignozzi, C. A.; Grätzel, M. *J. Am. Chem. Soc.* **2001**, *123*, 1613; (d) Grätzel, M. *Inorg. Chem.* **2005**, *44*, 6841.
3. (a) Wang, Z.-S.; Cui, Y.; Hara, K.; Dan-oh, Y.; Kasada, C.; Shinpo, A. *Adv. Mater.* **2007**, *19*, 1138; (b) Hara, K.; Miyamoto, K.; Abe, Y.; Yanagida, M. *J. Phys. Chem. B* **2005**, *109*, 23776.
4. Kuang, D.; Uchida, S.; Humphry-Baker, R.; Zakeeruddin, S. M.; Grätzel, M. *Angew. Chem., Int. Ed.* **2008**, *47*, 1923.
5. (a) Ehret, A.; Stuhl, L.; Spitler, M. T. *J. Phys. Chem. B* **2001**, *105*, 9960; (b) Sayama, K.; Hara, K.; Ohga, Y.; Shinpou, A.; Suga, S.; Arakawa, H. *New J. Chem.* **2001**, *25*, 200.
6. Sayama, K.; Tsukagoshi, S.; Hara, K.; Ohga, Y.; Shinpou, A.; Abe, Y.; Suga, S.; Arakawa, H. *J. Phys. Chem. B* **2002**, *106*, 1363.
7. (a) Yao, Q.-H.; Shan, L.; Li, F.-Y.; Yin, D.-D.; Huang, C.-H. *New J. Chem.* **2003**, *27*, 1277; (b) Yao, Q.-H.; Meng, F.-S.; Li, F.-Y.; Tian, H.; Huang, C.-H. *J. Mater. Chem.* **2003**, *13*, 1048.
8. (a) Eu, S.; Hayashi, S.; Umeyama, T.; Oguro, A.; Kawasaki, M.; Kadota, N.; Matano, Y.; Imahori, H. *J. Phys. Chem. C* **2007**, *111*, 3528; (b) Cid, J.-J.; Yum, J.-H.; Jang, S.-R.; Nazeeruddin, M. K.; Martínez-Ferrero, E.; Palomares, E.; Ko, J.; Grätzel, M.; Torres, T. *Angew. Chem., Int. Ed.* **2007**, *46*, 8358.
9. Chang, Y.-J.; Chow, T. J. *Tetrahedron* **2009**, *65*, 4726.
10. (a) Xu, M.; Li, R.; Pootrakulchote, N.; Shi, D.; Guo, J.; Yi, Z.; Zakeeruddin, S. M.; Grätzel, M.; Wang, P. *J. Phys. Chem. C* **2008**, *112*, 19776; (b) Li, R.; Lv, X.; Shi, D.; Zhou, D.; Cheng, Y.; Zhang, G.; Wang, P. *J. Phys. Chem. C* **2009**, *113*, 7469; (c) Mishra, A.; Fischer, M. K. R.; Bäuerle, P. *Angew. Chem., Int. Ed.* **2009**, *48*, 2474.
11. (a) Shen, P.; Liu, Y.; Huang, X.; Zhao, B.; Xiang, N.; Fei, J.; Liu, L.; Wang, X.; Huang, H.; Tan, S. *Dyes Pigments* **2009**, *83*, 187; (b) Cho, N.; Choi, H.; Kim, D.; Song, K.; Kang, M.-S.; Kang, S. O.; Ko, J. *Tetrahedron* **2009**, *65*, 6236; (c) Kim, D.; Song, K.; Kang, M.-S.; Lee, J.-W.; Kang, S. O.; Ko, J. *J. Photochem. Photobiol. A: Chem.* **2009**, *201*, 102.
12. (a) Choi, H.; Lee, J. K.; Song, K.; Kang, S. O.; Ko, J. *Tetrahedron* **2007**, *63*, 3115; (b) Chen, R.; Yang, X.; Tian, H.; Wang, X.; Hagfeldt, A.; Sun, L. *Chem. Mater.* **2007**, *19*, 4007; (c) Tian, H.; Yang, X.; Chen, R.; Zhang, R.; Hagfeldt, A.; Sun, L. *J. Phys. Chem. C* **2008**, *112*, 11023.
13. (a) Thomas, K. R. J.; Hsu, Y.-C.; Lin, J.-T.; Lee, K.-M.; Ho, K.-C.; Lai, C.-H.; Cheng, Y.-M.; Chou, P.-T. *Chem. Mater.* **2008**, *20*, 1830; (b) Lin, J.-T.; Chen, P.-C.; Yen, Y.-S.; Hsu, Y.-C.; Chou, H.-H.; Yeh, M. C. P. *Org. Lett.* **2009**, *11*, 97; (c) Chen, K.-F.; Hsu, Y.-C.; Wu, Q.; Yeh, M. C. P.; Sun, S.-S. *Org. Lett.* **2009**, *11*, 377.